Influence of the three-dimensional effects on the simulation of landscapes in thermal infrared

Thierry Poglio, Eric Savaria, Lucien Wald

Influence of the three-dimensional effects on the simulation of landscapes in thermal infrared.

T. Poglio
System Architecture Division, Alcatel Space, Cannes-la-Bocca, France; Groupe Télédétection & Modélisation, Ecole des Mines de Paris, Sophia Antipolis, France

E. Savaria
System Architecture Division, Alcatel Space, Cannes-la-Bocca, France

L. Wald
Groupe Télédétection & Modélisation, Ecole des Mines de Paris, Sophia Antipolis, France

ABSTRACT: The paper deals with the modelling of landscapes for the simulation of very high spatial resolution images in the thermal infrared range, from 3 to 14 µm. It focuses on the influence of the 3-D effects on the simulation. The major relevant physical processes are described. Examples are made, comparing simulations obtained with 2-D and 3-D representation of the landscape. They help in classifying the relative influence of each process. The necessity to take into account a 3-D landscape representation for the simulation of very high spatial resolution images in the infrared range is also demonstrated.

1 INTRODUCTION

There is a large demand of very high spatial resolution imagery in the infrared range in many and various fields, like meteorology, farming or military information. Such imagery with a spatial resolution of a meter or so is not yet available but new spaceborne systems are under development. Critical points are the assessment of the capacity of such systems and users training to the use of such imagery. The simulation is a crucial tool in this respect. It helps to reproduce the characteristics of the observing system. The output is a simulated image such as it would be delivered by the system. An essential point of the simulation of the observing system is an accurate knowledge of the input parameters, which are provided by a simulator of landscapes.

Variable meteorological conditions, different places, different landscapes, different times and different spectral bands should be simulated. A landscape synthesis method has been selected in order to meet better these requirements. In thermal infrared, the flux coming from an object is partly emitted by the object because of its own temperature, and partly due to the reflection of incident rays on the surface of this object. Depending on the surface material and the spectral band, emission or reflection process dominates the signal. For each object in the scene, the landscape simulator predicts the heat exchanges between objects, the temporal evolution of heat balance, the spectral emission and the spectral reflection of all incident fluxes.

For remotely sensed images, the influence of the relief depends on the ratio between the characteristic height of objects and the sampling rate of the image. Given the very high spatial resolution of the simulated landscape, we shall study impacts of this 3-D description on the synthesised image.

Jaloustre-Audouin (1998) and Jaloustre-Audouin *et al.* (1997) have developed a simulator of any type of landscape in 2-D. It models very efficiently the physical behavior of the objects taken separately. Image simulators with 3-D landscape representations as input exist, but only for specific application like thermal behavior of vehicles (Johnson *et al.*, 1998) or radiative budget modeling for vegetated areas (Guillevic, 1999).

Physical processes playing a part in the signal coming from the scene are described in the first section. The following section presents the relevance of physical phenomena in a 3-D representation. Then, a quantification of these phenomena is proposed with help of examples, making comparisons between simulations obtained with 2 and 3-D representations. A classification of impact is proposed for the main relevant phenomena. Some other phenomena may have a noticeable impact but depend too much on the spectral range, the meteorological or geographical conditions to enter this general classification. Their impacts are discussed in regard with the condition of the simulation, especially with the spectral range. It is conclude that the image sampling rate is linked to the necessity of an adapted landscape representation for the very high spatial resolution image simulation in the infrared range.

2 THE PHYSICAL PROCESS

In thermal infrared, the flux coming from an object in a given spectral range is both due to its own temperature and to spectral reflection of incident fluxes in this range. Depending on the spectral band and the surface material, the emission or reflection process dominates the signal. So, both processes have to be computed carefully.

2.1 *Emitted flux*

The emitted flux or irradiance (in W.m^{-2}) in a given spectral range, from λ_1 to λ_2 is given by:

$$L^e_{\lambda_1\lambda_2}(\theta,\varphi) = \pi \int_{\lambda_1}^{\lambda_2} \varepsilon_s(\lambda,\theta,\varphi) L^{bb}(\lambda,T_s) d\lambda \quad (1)$$

$$L^{bb}(\lambda,T_s) = \frac{2 \cdot hc^2}{\lambda^5 \cdot \left[\exp\left(\frac{hc}{\lambda k T_s} \right) - 1 \right]} \quad (2)$$

where L^{bb} is the flux emitted by a blackbody; T_s the surface temperature; and (θ,φ) the angles of the viewing direction. h,c and k are respectively the Planck constant; the light velocity and the Boltzmann constant. The quantity ε_s is the spectral emissivity of the object.

Under the thermodynamical conditions usually encountered in landscapes, the heat equation may be written as:

$$\frac{\partial T_s}{\partial t} = \kappa \cdot \Delta T_s \quad (3)$$

where κ is the thermal diffusivity, *i.e.* the ratio between the thermal conductivity and the product of the material density by the specific heat. This equation may be solved using e.g., the finite difference method, knowing:

- the temperature at the previous moment,
- the deep temperature of the object,
- the flux balance at the surface of the object.

The two temperatures result from inertia phenomena, whereas flux balance is an instantaneous phenomenon. Large temperature variations are due to large changes in flux balance. The flux balance at the surface of an object is given by the difference between radiative and convective fluxes. This difference corresponds to the conductive flux within the depth of the object, which gives rise to variations in surface temperature.

Table 1 presents typically values of these different fluxes. Radiative fluxes are very dependent on hourly conditions; solar irradiance can go from 0 at night from 1000 W.m^{-2} at midday. Sudden change in solar irradiance very much impacts flux balance value, whereas longwave irradiance does not. Radiative losses depend on the 4th power of surface temperature; there are very large for high surface temperature (50 °C) and smaller for weak temperature (0 °C). Convective fluxes mainly depend on gradient temperature between air and ground, and wind velocity. In addition, heat latent flux is very dependent on the ground moisture and the difference between relative humidity of the atmosphere and the ground.

Table 1: typical possible values for different fluxes (W.m^{-2}) at 45 °N.

Radiative fluxes:	Day	Night
Solar flux (for normal radiance direction):	900	-
- diffuse component	140	-
- direct component	760	-
Longwave flux	410	210
Radiative losses	700	280
Convective fluxes:		
Sensible heat	600	-50
Latent flux	800	-100

2.2 *Reflected flux*

All incident fluxes coming from other objects in the scene have to be considered as potential sources. An object i reflects a part of the received radiations H_i of various origins:

- solar radiation,
- atmospheric emission,
- reflected and emitted radiations from the surrounding objects.

The flux RR_i reflected by the object i is given by:

$$RR_{i\ \lambda_1\lambda_2} = \pi \int_{\lambda_1}^{\lambda_2} \rho_i(\lambda,\theta,\varphi) H_i(\lambda,\theta,\varphi) d\lambda \quad (4)$$

For computational reasons, H_i is written as a sum of contributions ordered by the number of consecutive reflections. Assuming Lambertian reflection and isotropic emission:

$$H_i = B_i + \sum_{V_i} \rho_j F'_{ij} \left\{ B_j + ... \left\{ B_p + \sum_{V_p} \rho_q F'_{pq} B_q \right\} ... \right\} \quad (5)$$

$$F_{ij} = \xi_{ij} \cdot F'_{ij} \quad (6)$$

where B_i represents the different sources for the object i: solar radiation, atmospheric emission, and emission of the surrounding objects; ρ_i is the fraction of flux scattered or reflected; V_i is the environment of the object i; F_{ij} and ξ_{ij} are respectively the form factor and the transmission coefficient between the objects i and j.

It follows that the computation of the reflected flux received by an object requests the knowledge of the distribution and the orientation of the objects in the surrounding and their interactions.

3 2-D LANDSCAPE REPRESENTATION VERSUS 3-D

A 2-D representation of a very high spatial resolution scene disregards:

- solar shades; due to buildings, houses, trees…,
- wind disturbance around buildings,
- influence between objects: multiple reflections, heat conduction, obstructions of the horizon…,
- all the 2-D effects (especially humidity assessment) affected by those described as previous points.

Solar shade effect is certainly the natural effect giving the most important differences between a 2-D and a 3-D representation. In a 2-D representation, each object receives from the Sun the same solar global flux. The global flux is the sum of the direct and the diffuse components. The direct component expresses the flux coming directly from the Sun attenuated by the atmospheric path. The diffuse component corresponds to the part of radiation reflected, diffracted or diffused by molecules constituting the atmosphere and aerosols. The ratio of these two components is varying all the day long, mainly with the Sun elevation angle. This is illustrated in Figure 1, which displays the global irradiance and its components received on a horizontal plane without horizon obstruction. The simulation is made using the ESRA model (Rigollier *et al.*, 2000).

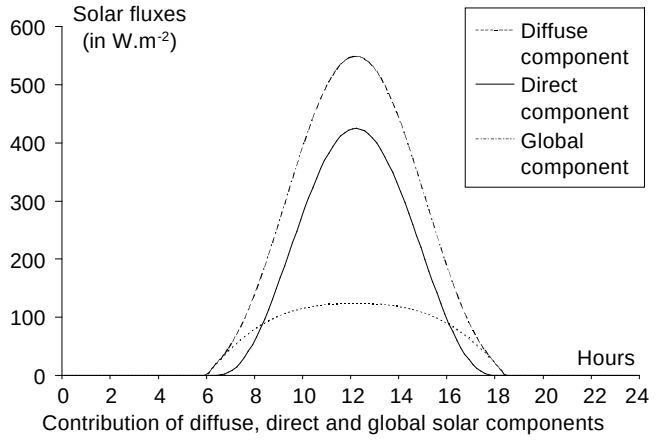

Figure 1: typical values of the different contributions of solar components for a horizontal object; the 21st of March, 45 °N.

Because the solar radiation is not isotropic, orientation between object and the Sun is also playing a role in the difference of solar fluxes balance between objects; 2-D representation cannot reproduce this reality. In addition, the diffuse radiation received by an object depends on the fraction of the sky dome, which is viewed from this object.

A shaded object will only receive a par of the diffuse component depending on the viewed fraction of the sky dome. Since its flux balance is generally negative in such a situation, its temperature will decrease, and its own emission too. Furthermore, because of the shadow, it will not reflect as much flux as if it was sunny. These two effects add to change considerably the global flux emitted by this object. Note that if this effect is very important it is nevertheless local, and does not affect more objects than the shaded ones.

In a 2-D description, the wind velocity is the same for each object. Reality is different, because each 3-D object disturbs the airflow. Solid objects, like houses or buildings, prevent wind from blowing with the same direction and velocity everywhere. This affects the entire scene; it is dependent on the distribution and the orientation of the objects in the scene. Since it is a convective effect, it only affects temperature of the object, and emitted flux as a consequence.

In a 2-D description there is no radiative interaction between objects. This is not true in 3-D. In the infrared range, each object acts both as a source and as a reflecting object. The assessment of the flux balance or the spectral emission coming from an object is highly dependent of its environment. A radiosity method (Watt, 2000; Sillion *et al.*, 1994) can be used to solve such a problem. In order to decrease the computational efforts, consideration of the physical processes help in reducing the environment V_i (eq. 5) of an object to a few objects in its nearest neighborhood. Among these processing is the decrease of the influence of an object onto another one as their distance increase. The low reflectance value also contributes to this decrease; for most objects it ranges from 0,05 to 0,3 (ASTER, 2000).

When two objects in different thermodynamical states are in contact, heat exchange occurs until equilibrium establishes. Heat exchange occurs from the warmest object to the coldest. A temperature gradient exists through the boundary, related to a gradient in emitted radiance. Heat conduction tends to reduce these gradients. In most cases, due to different boundary condition on each object, thermal equilibrium is not reached.

In a 3-D representation, two cases are observed where heat conduction plays a noticeable role:

- a temperature gradient exists between two materials. Such a gradient may arise from shading effects,
- the scene geometry permits local heat accumulation or local heat loss.

Considering a building with a north-oriented facade and a sun-drenched roof, heat conduction will process from the roof to the ground trough the facade, due to temperature gradient. Considering a house with a south-oriented corner, *i.e.* a south-east oriented facade and a south-west oriented one, it will

produce a heat accumulation in the corner all the day long and its temperature will locally increase.

Although differences of several degrees in temperature exist between situations simulated taking into account heat conduction or not, it only affects a small area. Expressed in terms of distance, even if flux balance is very different on both objects, an important temperature difference only exists on a few tens of centimeters. Considering or not heat conduction as an important phenomenon for infrared landscape simulation highly depends on the sampling rate expected for the final image. Available images in the infrared range taken at very high spatial resolution exhibit smooth temperature transitions. Hence simulation should reproduce such observations and heat conduction should be considered locally.

4 ILLUSTRATING THESE PHENOMENA WITH EXAMPLES

An example is given in order to illustrate our discussion. It is a grass ground, without rain during the simulation, on the 21st of March, at 45 °N, with relative moisture of 0,5 % for ground and 0,6 % for air. The wind is blowing at 1 $m.s^{-1}$, air temperature is oscillating between 7 and 18 °C. The albedo is 0,15 and the average emissivity integrated on the total spectral range is 0,84.

In accordance with the previous works and analyses made by Jaloustre-Audouin (1998), we used the following models. For the global radiative fluxes, models used were ESRA for solar radiation (Rigollier *et al.*, 1999), Swinbank for longwave radiation (*In* Jaloustre-Audouin, 1998), the blackbody function and average material emissivity for emission. A sensible heat model (Louis, 1979), and a latent heat model (Noilhan & Planton, 1989) were used for the prediction of convective fluxes. Spectral irradiance was assessed by the use of MODTRAN for solar radiation (Kneizys *et al.*, 1996) and the Berger's model (1988) was used for atmospheric radiation assessment.

Impacts of physical phenomena were studied in two spectral bands: band II from 3 to 5 µm, and band III from 8 to 12 µm. These two bands correspond to atmospheric windows, where the signal is the less affected by the atmosphere transmission. The spectral reflectance is given by the ASTER database (ASTER, 2000). Using the Kirchoff's law we assumed the spectral complementarity between emissivity and reflectance:

$$\varepsilon(\lambda,\theta,\varphi) = 1 - \rho(\lambda,\theta,\varphi) \qquad (7)$$

Although thermal equilibrium never occurs in the simulations for remote sensing applications (Salisbury, 1994), Kirchoff's law can be used to link spectral reflectance and emissivity without making noticeable errors (Korb, 1999).

In most cases, the physical effects combine in a complex manner and cannot be separated. For illustration, we selected cases for which this separation is possible.

4.1 *Solar shade effect*

Two situations corresponding to a 3-D representation of the landscape were simulated. The first one is the grass ground shaded from 9 to 12 h local solar time (LST) and the second one the grass ground shaded from 13 to 16 h LST. These simulations are compared to the simulation for a 2-D representation without shades. According to the ESRA model, the average diffuse solar component is respectively 25 % and 20 % of global irradiance for these two periods. These three simulations are shown in Figure 2 for band II and Figure 3 for band III.

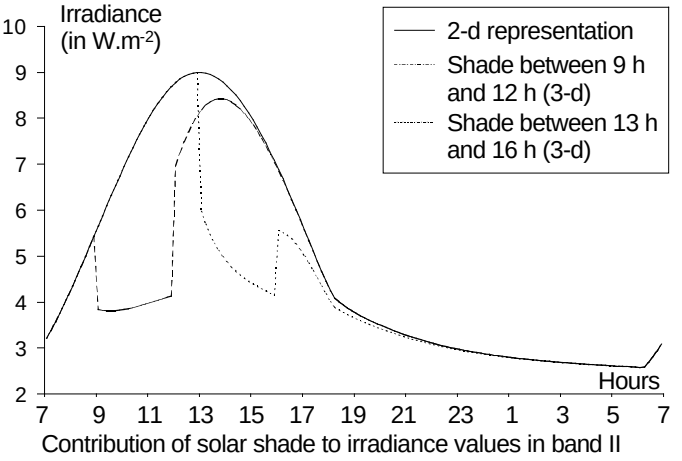

Figure 2: solar shade effects in band II. In full line, daily surface temperature evolution considering a 2-D representation. In dotted lines, the temperature evolution in two cases: a shading effect between 9 and 12 h and a shading one between 13 and 16 h LST.

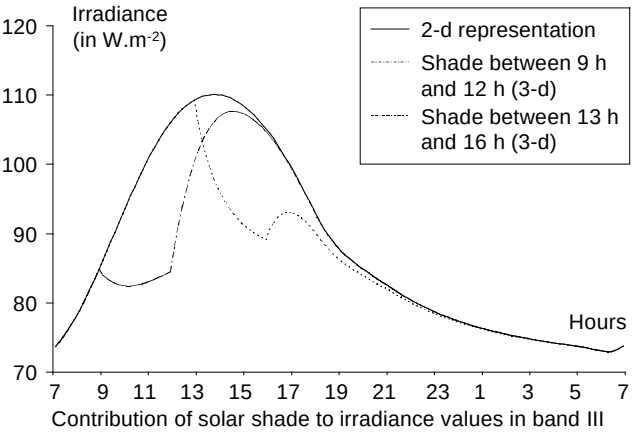

Figure 3: as Figure 2 but for band III.

For both bands, even if the irradiance values differ, the 2-D landscape representation approximation overestimates the irradiance. It not only occurs during the shaded time, but also in the following moments due to temperature inertia phenomenon. This

overestimation may be very important, especially if the shaded areas cover several pixels in the high resolution simulated image.

The following tables (Tables 2 and 3) present the average values obtained for 2-D and 3-D landscape representation.

Table 2: average temperature and irradiance values from 9 to 12 h LST in 3-D and 2-D landscape representation cases.

	Average temperature	Average irradiance in band II	Average irradiance in band III
Ground shaded (3-D representation)	12,6 °C	4,0 W.m^{-2}	83 W.m^{-2}
Ground without shade (2-D representation)	21,6 °C	7,2 W.m^{-2}	97 W.m^{-2}
Relative Increase	-	+ 80 %	+ 17 %

Table 3: average temperature and irradiance values from 13 to 16 h LST in 3-D and 2-D landscape representation cases.

	Average temperature	Average irradiance in band II	Average irradiance in band III
Ground shaded (3-D representation)	19,6 °C	4,8 W.m^{-2}	95 W.m^{-2}
Ground without shade (2-D representation)	28,2 °C	8,3 W.m^{-2}	108 W.m^{-2}
Relative Increase	-	+ 73 %	+15 %

In band II, spectral reflection of incident solar flux constitutes the main part of the signal. Thus, as shade affects both temperature and spectral reflections, it is in this spectral range that approximating 3-D by a 2-D representation causes the largest errors. The error is always larger than 70 % in this spectral band. In band III, relative errors are smaller than in band II, but absolute values of differences are not. Anyway, these gaps are very important and shades must be taken into account in high spatial resolution image simulation in this spectral range.

4.2 *Wind disturbance*

Wind velocity and direction are affected by the pattern of all objects building the scene. Wind velocity will decrease if the object is protected from windblow whereas it will probably increase in a street between buildings. A simulation was done with the same conditions than previously described. The wind velocity is set to 1, 3 and 8 m.s^{-1}. Irradiance values in band III are presented on Figure 4. The larger the wind velocity, the more the surface temperature behavior comparable with air temperature. In case of inaccurate estimation of the wind velocity, Figure 4, shows that the largest errors in predicting irradiance are reached for the highest surface temperature values. It can be explained by the fact that irradiance follow the blackbody law, and an increase of a degree at a high temperature (30 °C) has more impact on the irradiance than an increase of a degree for a small temperature (5 °C). The maximal difference between temperature and irradiance are observed at 14 h LST. These differences are presented in the Table 4.

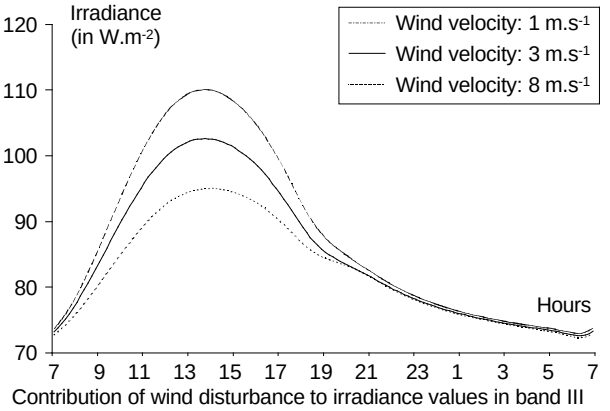

Figure 4: wind disturbance effects on irradiance values in band III.

Table 4: maximal temperature and irradiance values for different wind velocity.

Wind velocity (m.s^{-1})	Maximal temperature (°C)	Maximal irradiance in band II (W.m^{-2})	Maximal irradiance in band III (W.m^{-2})
1	29.1	9.0	110.1
3	24.6	8.2	102.6
8	19.8	7.5	95.1

Irradiance variations are not proportional to wind velocity. Particularly, irradiance is very sensible to wind velocity variations for small velocity. In band III, the difference is larger than 7 W.m^{-2} between a situation simulated with a wind velocity of 1 m.s^{-1} and 3 m.s^{-1}. It can be explained by the impact of the wind velocity on other phenomena. Not only wind velocity variations change sensible heat flux, but also latent heat flux and ground moisture. Without any precipitation during the simulation, ground will dry quicker under a strong wind than it will do under a light one. An accurate prediction of wind velocity on each object, *i.e.* an accurate prediction of velocity and direction of wind in the scene is necessary.

4.3 *Multiple reflections*

The aim here is to assess influence of object on each other. In this simulation, the landscape (Figure 5) is composed of three buildings enclosing a place. Walls of each building (objects n°1, 2 and 3) are made of construction concrete, and insulating material (polystyrene). The ground between buildings is in asphalt above earth. The simulation takes place on the 12th of October. Other simulation conditions are the same than in the previous example. Dimensions

indicated on the Figure 5 are such as: $c = 1.5d = 2a = 3b$. Emission and reflection of incident flux are presented in Table 5. The n^{th} order reflection for an object is computed by considering the $n\text{-}1^{th}$ reflections of its environment, *i.e.* all other objects, the atmosphere and the Sun.

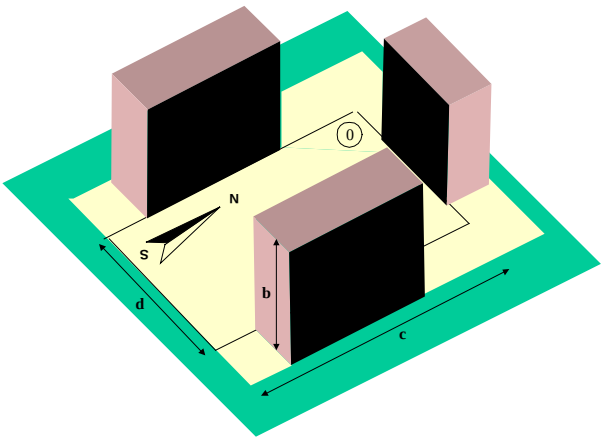

Figure 5: the scene considered in this example; the object 0 (framed) is the ground in asphalt, the objects 1, 2 and 3 are buildings. The interest for the simulation is the West-oriented facade of the building 1.

For each object, emission and reflected fluxes are computed. The interest here is the increase of global flux coming from an object, due to the computation of multiple reflections.

Table 5: emitted and reflected fluxes computed at order 1, 2 and 3 for the building 1. Contribution of current order compared with the sum of the previous ones (in percentage).

	Midnight		Midday	
Temperature	14,9 °C		21,6 °C	
Spectral flux ($W.m^{-2}$)	Band II	Band III	Band II	Band III
Emitted flux	3,34	93,09	4,32	104,52
Reflected flux; order 1	3,68 + 9,2 %	96,43 + 3,5 %	5,56 + 22,3 %	109,25 + 4,3 %
Reflected flux; order 2	3,69 + 0,3 %	96,49 + 0,1 %	5,62 + 1,6 %	109,33 + 0,1 %
Reflected flux; order 3	3,69 + 0 %	96,49 + 0 %	5,62 + 0 %	109,34 + 0 %

During the day, although it is illuminated by the Sun with nearly parallel incidence (due to azimuth angle at this date), reflected flux in band II represents 23 % of the global flux coming from the building n° 1. Compared to global flux, 77 % of the flux coming from the building is due to emission, 22 % is due to reflection computed at the first order, and 1 % is due to reflection computed at the second order. More generally, the first order for reflection is the most important whatever are time and spectral bands. Contribution of a given order in reflected flux decreases with the increase of the order of diffusion. In band III, computing reflected flux at the first order of diffusion might be enough. This is due to the very small influence of solar incident irradiance in this spectral range. In band II, the second order represents only about 1 % of the global flux. Nevertheless, it represents approximately $1/50^{th}$ of irradiance given in Table 2 or 3. It is a significant value with respect to the encoding properties of the envisioned observing system.

Multiple reflections are nevertheless very dependent on the spectral reflectance. In the example above, for the concrete construction, average reflectances are about 11 % in band II and 6 % in band III. Other materials may have larger reflectance values. For such cases, multiple reflections become noticeable; computing reflections at the first order of diffusion during the night and the second order during the day is necessary.

Another effect due to multiple reflection will appear in the interpretation of the images. During the night, the asphalt ground and the building number 2 are the warmest in the scene. There are also neighbors to buildings 1 and 3. The contributions of objects 0 and 2 to the flux emitted by the object 1 and 3 will reduce the differences between the buildings 2 and 1 (or 2 and 3), which would have been observed without the multiple reflections. This renders the accurate assessment of the actual temperature of each building more difficult.

5 CLASSIFICATION OF THE IMPACT OF PHYSICAL PHENOMENA ON THE SIMULATION

The approximation made by using a 2-D instead of a 3-D representation leads to errors that depend upon the considered physical phenomenon and its local relevance. For example, the wind effects will be found everywhere while the heat conduction will be noticeable for a few objects in a limited distance to their boundary. In another example, not only buildings can shade the ground, but they can also decrease the wind velocity. If these two effects add, simulations considering or not 3-D representation will differ drastically. On the contrary, combined influence of phenomena like multiple reflections, obstruction of the horizon or heat conduction can be null. Nevertheless, a classification of the impact of the physical phenomena can be performed by considering the average influence in a typical case of interest, such as an urban area. This classification is given in Table 6.

Table 6: classification (order of importance) of the impacts of the main physical phenomena influencing the simulation.

	Percentage
Solar shade effect	80 %
Wind disturbance around 3-D objects	20 %
Multiple reflections Horizon obstructions Heat Conduction	$\}$ ≅ 2 %

The percentages are only indicative. As a whole, the shade affects are predominant, followed by the

wind disturbances. Temperature of a given material expresses recent past of flux balance at the surface of the object including shade effects. Not only these effects are important at a given time, but also in a near future because of inertia phenomenon. So, the careful computation of shades has to be done all along the simulation. Though it only affects temperature and emitted flux, an accurate wind velocity modeling is also necessary, especially if the simulation has to be done during the night, when solar flux contribution is null. Phenomena directly attached at the environment of an object are more difficult to classify, because far too dependant on the simulation conditions. Without any particular knowledge of the simulation conditions they have to be taken into account. But, two criteria can be applied. If image simulation have to be done for thermal wavelengths (about 10 µm), computation of multiple reflections is usually not necessary. If the final image sampling rate is about a few meters the simulation of heat conduction between objects will not carry out a lot additional information and is not necessary.

6 CONCLUSION

In image simulation, as the sampling rate increases, realistic representation of the landscape is only possible with a 3-D representation. In this respect, objects that build the landscape interact each other. Realistic image simulation will have to reproduce faithfully these physical interactions between objects. In the infrared range, the main physical phenomena affecting the signal emitted by the scene are shade effect, wind disturbance linked to landscape relief, and depending on the simulation conditions, multiple reflections or heat conduction. Consequently, results presented here will be used as a starting point in the specification, the design and the development of a simulator of landscapes in the thermal infrared range with a very high spatial resolution.

REFERENCES

ASTER, 2000. ASTER spectral library Ver 1.2, CD-ROM, Jet Propulsion Laboratory, NASA, October 2000, http://spectib.jpl.nasa.gov/archive/jhu.html.

Berger X., 1988. A simple model for computing the spectral radiance of clear skies. *Solar Energy*, **40**, n°4, 321-333.

Guillevic P., 1999. *Modélisation des bilans radiatif et énergétique des couverts végétaux*. Thèse de Doctorat, Université P. Sabatier, Toulouse, France, 181 pp.

Jaloustre-Audouin K., 1998. *SPIRou : Synthèse de Paysage en InfraRouge par modélisation physique des échanges à la surface*. Thèse de Doctorat, Université de Nice-Sophia Antipolis, Nice, France, 169 pp.

Jaloustre-Audouin K., Savaria E., Wald L., 1997. Simulated images of outdoor scenes in infrared spectral band, *AeroSense'97*, SPIE, Orlando, USA.

Johnson K., Curran A., Less D., Levanen D., Marttila E., Gonda T., Jones J., 1998. MuSES: A new heat and signature management design tool for virtual prototyping, *Proceedings of the 9th Annual Ground Target Modelling & Validation Conference*, Houghtoon, MI.

Korb A.R., Salisbury J.W., D'Aria D.M., 1999. Thermal-infrared remote sensing and Kirchoff's law. 2. Fields measurements. *Journal of Geophysical Research*, **104**, 15,339-15,350.

Kneizys F.X., Shettle E.P., Gallery W.O., Chetwind J.H., Abreu L.W., Selby J.E., Clough S.A., Fenn R.W., 1988. *Atmospheric transmittance/radiance: computer code LOWTRAN 7* (AFGL-TR-88-0177), Hanscom AFB Massachusetts, Air Force Geophysics Laboratories, USA.

Louis J.-F., 1979. A parametric model of vertical eddy fluxes in the atmosphere. *Boundary Layer Meteorology*, 17, 187-202.

Noilhan J., Planton S., 1989. A simple parametrization of land surface processes for meteorological models. *Monthly Weather Reviews*, **117**, 536-549.

Rigollier C., Bauer O., Wald L., 2000. On the clear sky model of the ESRA - European Solar Radiation Atlas - with respect to the Heliosat method. *Solar Energy*, **68**, n°1, 33-48.

Salisbury J.W., Wald A., D'Aria D.M., 1994. Thermal-infrared remote sensing and Kirchoff's law. 1. Laboratory measurements. *Journal of Geophysical Research*, **99**, 11,897-11,911.

Sillion F.X., Puech C., 1994. *Radiosity & Global Illumination*. Morgan Kaufmann Publishers, Inc., ISBN 1-558-60277-1, San Francisco, CA, U.S.A., 251 p.

Watt A., 2000. *3-D Computer Graphics*, Third Edition, Addison-Wesley Publishing Compagny Inc, ISBN 0-201-39855-9.